ISSN 1392–1207. MECHANIKA. 2016 Volume 22(6): 553–561

Substantiation of concave crossbars shape for corn ears threshing

E. Pužauskas*, D. Steponavičius, E. Jotautienė***, S. Petkevičius****, A. Kemzūraitė*******
**Institute of Agricultural Engineering and Safety, Aleksandras Stulginskis University, Studentų 15A, 53362 Akademija, Kaunas distr., Lithuania, E-mail: e.puzauskas@hotmail.com*
***Institute of Agricultural Engineering and Safety, Aleksandras Stulginskis University, Studentų 15A, 53362 Akademija, Kaunas distr., Lithuania, E-mail: Dainius.Steponavicius@asu.lt*
****Institute of Agricultural Engineering and Safety, Aleksandras Stulginskis University, Studentų 15, 53362 Akademija, Kaunas distr., Lithuania, E-mail: Egle.Jotautiene@asu.lt*
*****Institute of Agricultural Engineering and Safety, Aleksandras Stulginskis University, Studentų 15A, 53362 Akademija, Kaunas distr., Lithuania, E-mail: Sigitas.Petkevicius@asu.lt*
******Institute of Agricultural Engineering and Safety, Aleksandras Stulginskis University, Studentų 15A, 53362 Akademija, Kaunas distr., Lithuania, E-mail: Aurelija.Kemzuraite@asu.lt*

crossref http://dx.doi.org/10.5755/j01.mech.22.6.16370

1. Introduction

The total land area cultivated with corn amounts to 178 million ha worldwide, and the total corn grain production amounts to approximately one billion tons annually. The EU countries produce approx. 75 million tons of corn grain annually [1]. Some countries, including Lithuania, practising the application of modern technologies in agriculture have been noted to use combine harvesters with a tangential, longitudinal axial flow, and tangential-longitudinal axial flow threshing devices for corn grain harvesting [2]. Nonetheless, frequent unfavourable meteorological conditions and the ineffectiveness of the combine structure under the respective conditions often result in grain harvest processing losses above the permissible thresholds [2, 3]. The reasons mentioned above imply the need for improvement of the threshing unit design on the basis of a detailed analysis of the process of corn ear threshing [4]. The corn threshing process taking place in a combine harvester threshing unit is a complex process of contact interaction between thresher mechanical parts and corn ears, including extrusion, collision, rubbing, etc. [5]. The threshing process is determined by the corn variety, design of the threshing unit, and its adjustment [6]. One of the key design parameters of a threshing unit critical for corn ear threshing is the shape, height, number of the concave crossbars and the position of the crossbar relative to the cylinder, as well as the active separation area of the concave [6, 7]. The concave is required to support the crop material passing through the threshing unit, so that the cylinder rasp bars can thresh the grain, and it must allow passage of the maximum possible amount of threshed grain [7]. Modern combine harvesters use concaves with rectangular crossbars for grain crops and rounded crossbars for corn. The concave wrapping radius is a constant, meaning that the clearance between the cylinder rasp bar and concave crossbars is subject to uneven variation. For the higher intensity of processes in the threshing unit as mentioned above, a variable radius concave has been designed, manufactured, tested and patented. The variable radius concave provides flexibility in terms of the number of crossbars, i.e. it allows changing the step of crossbars in the concave and their surface shape [8]. Previous studies have demonstrated that the variable radius concave improves the efficiency of corn grain separation through the concave grating by 2.5 [9]. The authors have asserted that application of that particular concave results in less damage to the grains. In addition, they suggest that further studies are required for optimisation of the crossbar surface shape and their step.

A series of studies presenting findings on the effect of threshing cylinder rotation speed, clearance between the cylinder and concave, feed rate of corn ears and moisture content of the corn ears on the qualitative and quantitative parameters of the corn ear threshing process have been published in the references [7, 10, 11]. Still, there is lack of studies considering the effect of the shape of concave crossbars on the damage and separation of corn grains. Most of the studies dealing with corn threshing have only been based on experiments, and there is lack of analysis of the interaction between the threshing cylinder rasp bar, concave bar, and the corn ear. The mechanism of these interactions is unclear, as a corn ear is a complex biological body characterised by its complex geometrical shape. The background review of literature has provided little information concerning the concave bars' design and its influence on grain separation and damage during the threshing process.

Hypothesis of the paper. The shape of the concave crossbars has a significant effect on the separation of grains from the corn cob, grain separation through the concave and grain damage during the threshing process.

2. Theoretical analysis

It is assumed that corn ears are pushed down the bottom *2* of a feeder conveyor *1* by the slats *3*, with the longitudinal axis of the ears being parallel to the slats (Fig. 1). As a result, the majority of the ears enter the clearance between the cylinder rasp bar *8* and the concave crossbar *5* positioned in parallel to the rasp bars. The threshing of corn ears fed at the first concave crossbar *5* is often inefficient due to the lack of sufficient support for the corn ears. Moreover, corn ears, which have entered the cavity between the rasp bars, are immediately passed to the second concave crossbar *6*, i.e. they usually have no contact with the first crossbar. For the reasons mentioned above, the theoretical analysis of the cylinder rasp bar, corn ear and concave is performed for the second concave crossbar. The entire corn ear threshing process is known to depend on the efficiency of the interaction between the

first cylinder rasp bar and the corn ear [12].

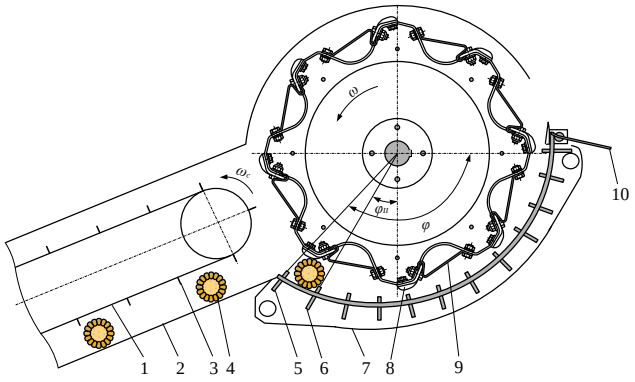

Fig. 1 Corn ear threshing unit: *1* - feeder conveyor; *2* - feeder house bottom; *3* - slats; *4* - corn ear; *5*, *6* - the first and second concave crossbars; *7* - concave; *8* - cylinder rasp bars; *9* - cylinder filler plates; *10* - rod grating; φ - concave wrapping angle ($\varphi = 130°$); φ_{II} - angle of the second concave crossbar relative to the vertical ($\varphi_{II} = 30°$); ω - angular velocity of the cylinder; ω_c - angular velocity of the feeder conveyor

In contrast to conventional combine harvesters, the concave covering the cylinder is not circular, but has a variable radius, similar to an Archimedean spiral. This type of concave has been validated by respective research studies and patented [8]. The theoretical analysis has been conducted by analysing the crossbars of three different shapes (Fig. 2), which are installed in the variable radius concave referred to above.

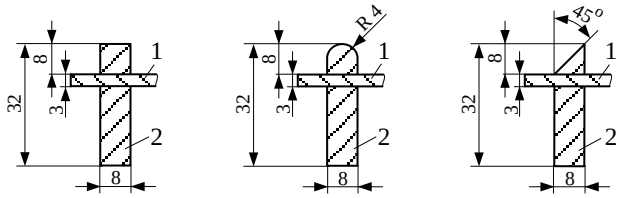

Fig. 2 Concave crossbars: *a* - rectangular; *b* - rounded; *c* - oblique; *1* - concave rod; *2* - concave crossbar

Traditional continuum mechanics analysis methods can be applied to analyse the force applied to a single corn ear, cob, and grain in the corn threshing process [13]. The analytical study of the threshing process under this research involves the application of a Ø46 mm corn ear *II*, which interacts with a Ø0.8 m threshing cylinder rasp bar *I* and the second concave crossbar *III* (Fig. 3). The corn cob is surrounded by 14 grains at any of its cross-sections; single grain height – 9 mm, width – 8.4 mm. Three accurate process calculation schemes have been developed for the static equilibrium study in order to determine the numeric values of the reaction forces (only the structure of an oblique concave crossbar is depicted in Fig. 3). Force P is applied to the grain by the striking rasp bar. This force tends to push the grain toward the centre of the ear (force P_n), simultaneously rotating the ear in the clockwise direction and moving it in a lateral direction to the right (force P_τ). The corn ear bottom rests with a single grain on the concave rod *IV* and crossbar *III*. Reaction forces N_2 and N_1 are applied to these contact points. The process of detaching the corn grains from their supporting structure, the cob, is defined as shelling or threshing. Shelling occurs when the forces applied to the grains overcome the holding strength of the grain attachment to the cob. In addition, the corn cob reaction to grain force N_{22} and grain reaction to grain forces N_{12} are applied.

The active friction forces are expressed as the multiplication of the normal reaction forces and friction coefficients: $F = f_1 P_n$; $F_{N1} = f_1 N_1$; $F_{N2} = f_2 N_2$; $F_{N12} = f_2 N_{12}$; $F_{N22} = f_3 N_{22}$. The friction coefficients f_1 between the corn grain and steel section of the working tool of the threshing unit are equal to 0.33, friction coefficients between the contacting grains $f_2 = 0.25$, and the grain to corn cob friction coefficients $f_3 = 0.42$ [12].

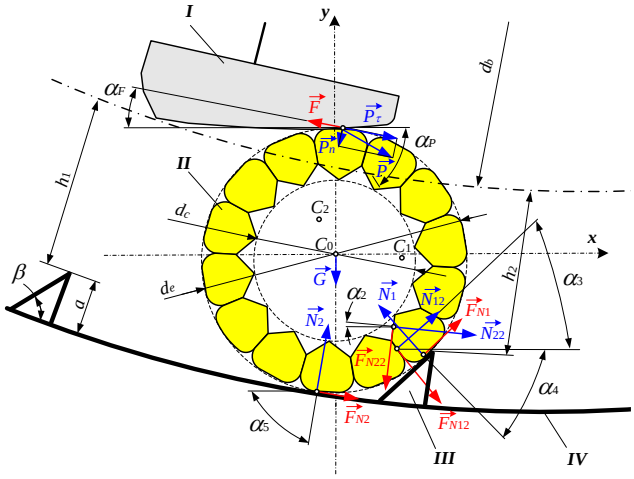

Fig. 3 Interaction between the rasp bar, corn ear and second concave crossbar: *I* - cylinder rasp bar; *II* - corn ear; *III* - the second concave crossbar; *IV* - concave rod; C_0, C_1, C_2 - points referred to by the equations of the moments of force; a - height of the concave crossbars ($a = 8$ mm); h_1, h_2 - distances of the rasp bar to the first and second concave crossbars ($h_1 = 36$ mm, $h_2 = 34$ mm); d_b, d_e, d_c - diameters of the cylinder, corn ear and corn cob ($d_b = 800$ mm, $d_e = 46$ mm, $d_c = 28$ mm); β - tilt angle of the working plane of the concave crossbars ($\beta = 45°$); (other designations are provided in Table 1)

The four equilibrium equations with 4 unknowns are composed. For this purpose, the acting forces are expressed on the x and y axes of the coordinate system:

$$\sum F_x = P\cos\alpha_P - F\cos\alpha_F + N_{22}\cos\alpha_2 - F_{N22}\sin\alpha_2 + N_{12}\cos\alpha_3 + F_{N12}\sin\alpha_3 - N_1\cos\alpha_4 + F_{N1}\sin\alpha_4 + N_2\cos\alpha_5 + F_{N2}\sin\alpha_5 = 0; \quad (1)$$

$$\sum F_y = -P\sin\alpha_P + F\sin\alpha_F - G - N_{22}\sin\alpha_2 - F_{N22}\cos\alpha_2 + N_{12}\sin\alpha_3 - F_{N12}\cos\alpha_3 + N_1\sin\alpha_4 + F_{N1}\cos\alpha_4 + N_2\sin\alpha_5 - F_{N2}\cos\alpha_5 = 0. \quad (2)$$

In addition, the moments of the acting forces have been written down for the chosen points C_1 and C_2:

$$\sum M_{C1} = -Pl_{PC1} + Fl_{FC1} + Gl_{GC1} + N_{22}l_{N22C1} - F_{N22}l_{FN22C1} + N_{12}l_{N12C1} + F_{N12}l_{FN12C1} - N_1l_{N1C1} + \\ + F_{N1}l_{FN1C1} - N_2l_{N2C1} + F_{N2}l_{FN2C1} = 0; \quad (3)$$

$$\sum M_{C2} = -Pl_{PC2} + Fl_{FC2} - Gl_{GC2} + N_{22}l_{N22C2} - F_{N22}l_{FN22C2} + N_{12}l_{N12C2} - F_{N12}l_{FN12C2} - N_1l_{N1C2} + \\ + F_{N1}l_{FN1C2} + N_2l_{N2C2} + F_{N2}l_{FN2C2} = 0. \quad (4)$$

The angles of all the forces marked in Fig. 3 and distances to points C_0, C_1 and C_2 have been calculated using the AutoCAD 2006 application (Table 1). The table also contains data of the other two structures (for rectangular and rounded crossbars).

Table 1

Model values (see Fig. 3)

Indicator	Designation, dimension	Crossbar shape		
		rounded	rectangular	oblique
Rasp bar force acting on the corn ear grain	P, N	32.00	32.00	32.00
Force P components:				
tangential	P_τ, N	31.36	31.41	31.31
normal	P_n, N	6.35	6.14	6.62
Rasp bar to corn ear grain friction force	F, N	2.09	2.03	2.18
Corn ear gravity force	G, N	3.92	3.92	3.92
Angle of the rasp bar force P acting on the grain relative to the horizontal	α_P, °	23.00	23.00	23.00
Force F angle relative to the horizontal	α_F, °	11.55	11.94	11.07
Angle of the corn cob reaction to grain force N_{22} relative to the horizontal	α_2, °	26.54	21.14	16.43
Angle of the grain reaction to grain force N_{12} relative to the horizontal	α_3, °	21.00	21.00	25.71
Angle of the concave crossbar reaction to grain force N_1 relative to the horizontal	α_4, °	52.29	45.00	45.00
Angle of the concave rod reaction to grain force N_2 relative to the horizontal	α_5, °	84.47	79.38	70.48
Distance between force P vector and parallel straight line crossing point:				
C_0	l_{PC0}, mm	22.47	22.38	22.50
C_1	l_{PC1}, mm	19.06	18.97	19.10
C_2	l_{PC2}, mm	18.88	18.79	18.92
Distance between force F vector and parallel straight line crossing point:				
C_0	l_{FC0}, mm	22.92	22.80	23.00
C_1	l_{FC1}, mm	21.45	21.26	21.61
C_2	l_{FC2}, mm	18.31	18.22	18.35
Distance between force G vector and parallel straight line crossing point:				
C_0	l_{G0}, mm	0	0	0
C_1	l_{G1}, mm	9.99	9.99	9.99
C_2	l_{G2}, mm	3.68	3.68	3.68
Distance between force N_{22} vector and parallel straight line crossing point:				
C_0	l_{N22C0}, mm	9.23	10.16	10.35
C_1	l_{N22C1}, mm	13.21	13.26	12.66
C_2	l_{N22C2}, mm	12.47	13.92	14.55
Distance between force F_{N22} vector and parallel straight line crossing point:				
C_0	l_{FN22C0}, mm	11.47	12.19	11.47
C_1	l_{FN22C1}, mm	1.95	2.68	1.73
C_2	l_{FN22C2}, mm	16.87	17.60	16.55
Distance between force N_{12} vector and parallel straight line crossing point:				
C_0	l_{N12C0}, mm	18.43	18.78	18.43
C_1	l_{N12C1}, mm	14.35	14.69	13.61
C_2	l_{N12C2}, mm	24.85	25.19	24.95

Table 1 (Continued)

Indicator	Designation, dimension	Crossbar shape		
		rounded	rectangular	oblique
Distance between force F_{N12} vector and parallel straight line crossing point:				
C_0	l_{FN12C0}, mm	0	0.67	0
C_1	l_{FN12C1}, mm	9.13	8.47	8.77
C_2	l_{FN12C2}, mm	1.48	2.15	0.95
Distance between force N_1 vector and parallel straight line crossing point:				
C_0	l_{N1C0}, mm	0.45	1.52	0.78
C_1	l_{N1C1}, mm	8.02	8.21	7.46
C_2	l_{N1C2}, mm	0.87	2.78	2.03
Distance between force F_{N1} vector and parallel straight line crossing point:				
C_0	l_{FN1C0}, mm	22.94	23.41	23.00
C_1	l_{FN1C1}, mm	16.40	15.96	15.55
C_2	l_{FN1C2}, mm	29.52	29.88	29.46
Distance between force N_2 vector and parallel straight line crossing point:				
C_0	l_{N2C0}, mm	2.72	0.46	0.23
C_1	l_{N2C1}, mm	12.71	10.38	10.16
C_2	l_{N2C2}, mm	1.48	4.17	4.30
Distance between force F_{N2} vector and parallel straight line crossing point:				
C_0	l_{FN2C0}, mm	22.81	22.91	23.00
C_1	l_{FN2C1}, mm	23.24	24.22	24.11
C_2	l_{FN2C2}, mm	27.89	27.60	27.77

The solution of Eqs. (1)-(4) under the numerical method using the Maple14 application provides the numerical values of the forces under consideration (Table 2).

Static verification is then conducted by writing down the equations of the moments of the acting forces for point C_0:

$$\sum M_{C0} = -Pl_{PC0} + Fl_{FC0} + N_{22}l_{N22C0} - F_{N22}l_{FN22C0} + N_{12}l_{N12C0} - F_{N12}l_{FN12C0} - \\ - N_1 l_{N1C0} + F_{N1}l_{FN1C0} - N_2 l_{N2C0} + F_{N2}l_{FN2C0} = 0. \quad (5)$$

The theoretical analysis has demonstrated that oblique concave crossbars provide maximum numerical values of the force N_1 of the concave crossbar reaction to grain and force N_{12} of the grain reaction to grain. This suggests that the threshing process using oblique crossbars would probably be more efficient that using any of the other two shapes of crossbars.

Table 2

Calculated numerical values of the reaction forces

Indicator	Designation, dimension	Crossbar shape		
		rectangular	rounded	oblique
Force of the concave crossbar reaction to grain	N_1, N	192.70	73.47	252.48
Force of the grain reaction to grain	N_{12}, N	-72.85	24.24	-140.37
Force of the concave rod reaction to grain	N_2, N	-16.18	-62.25	-0.93
Force of the corn cob reaction to grain	N_{22}, N	187.65	0.0007	278.98

Further analysis using Eqs. (1-4) has been conducted to determine the dependences of forces N_1 and N_{12} acting on the grain on the tilt angle of the working plane of the crossbars β (Fig. 4). The larger the angle β, the greater the numerical values of forces N_1 and N_{12}. This means that the grains contained in the corn ear are subjected to more intensive action at the second concave crossbar, and the conditions for their detachment from the corn cob are more favourable. The further increase of the angle is restricted by the force which, when acting on the grains, causes damage to their outer hulls. Depending on the grain maturity and moisture content, the force has been found to range up to 200.67 ± 18.43 N. Hence, in conclusion to the theoretical analysis, the working plane tilt angle of the concave crossbar β could be suggested from 35° to 40°.

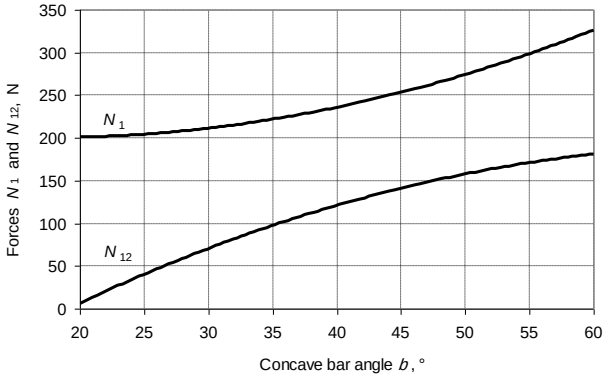

Fig. 4 Dependence of the moduli of forces N_1 and N_{12} acting on the grain on the working plane tilt angle of the crossbar β

Calculation of the displacement of individual corn ear parts using the finite element method. Due to rapid developments in computer hardware and software in recent decades, some numerical methods have been used in many industrial and agricultural fields [14]. The finite element method (FEM) has been used widely in agricultural machinery in the recent decades. Xu et al. [15] stated that the mechanism of rice impact damage is unclear. As a result, they examined the interaction between the threshing tooth and the rice kernel using FEM analysis. The FEM model of rice kernel was established after specifying material properties. Simulation and analysis of the impact between the threshing tooth and the rice kernel were performed. Simulations showed that the critical velocity of impact damage corresponding to the critical tensile stress of the rice kernel was 29.5 m s^{-1} [15]. Nowadays, the promising discrete element method (DEM) is also widely used as a tool to predict the behaviour of particulate assemblies [14]. Application of the DEM requires that the corn grain surface be described as subspherical shapes. The authors have analysed approximations of 4, 6, 8 and 12 subspheres [14]. Three-dimensional DEM and software can be used to analyse the threshing process and optimize the corn thresher or corn combine harvester without any need to undertake extensive bench tests [13]. The researchers have applied this method to analysis of the drum corn ear thresher widely used only in China under the stationary mode, but the thresher is significantly different from the tangential threshing unit considered in this paper.

For this paper in particular, the displacement, deformation and stress values, as well as the values of other processes happening inside a deformable corn ear, are calculated using the FEM. Whereas the surfaces of corn ear parts are not even, curved finite elements, i.e. second order curved rectangular isoparametric finite elements are used. These particular finite elements allow for a highly accurate approximation of a curved surface [16].

Curved elements are also subject to the principle of displacement compatibility at edges and the continuity principle. Curved elements may be generated by reorganising the elements already available in the local system into the curvilinear coordinate system. The following mathematical relationship exists between any points of the element in both coordinate systems:

$$\left.\begin{aligned} x &= \left[N_1(\xi,\eta), N_2(\xi,\eta)\ldots \right] \begin{Bmatrix} x_1 \\ x_2 \\ \vdots \end{Bmatrix}; \\ y &= \left[N_1(\xi,\eta), N_2(\xi,\eta)\ldots \right] \begin{Bmatrix} y_1 \\ y_2 \\ \vdots \end{Bmatrix}, \end{aligned}\right\} \quad (6)$$

where N_i are the element shape functions (interpolation polynomials) in the local system $\xi 0 \eta$, while x_i and y_i - coordinates of the element nodes in the global system.

Quadrilateral second order isoparametric finite elements of the Serendip type have been chosen for approximation of the corn ear parts.

Functional dependence (6) has allowed determining which point (x, y) of the curved element in the global system corresponds to the point (ξ, η) chosen inside the element in the local system. It can be used to link the element node coordinates in the local system with the respective element node coordinates in the global system.

In this case, the shape function derivatives with reference to x and y are calculated under the formula:

$$\left[N'_{x,y} \right] = \left[J \right]^{-1} \left[N'_{\xi,\eta} \right]. \quad (7)$$

The element stiffness matrix is calculated under the formula:

$$\left[K^e \right] = \int_{-1}^{1} \int_{-1}^{1} \left[B(\xi,\eta) \right]^T \left[D \right] \left[B(\xi,\eta) \right] det\left[J \right] d\xi d\eta \,, \quad (8)$$

where $[B]$ - matrix of the shape function derivatives; $[D]$ - matrix of mechanical properties of the material; $[J]$ - Jacobian matrix; ξ, η - shape function matrix in the local coordinate system.

A corn ear is split into 28 isoparametric finite elements with 8 nodes (Fig. 5). Number of nodes is 127. Each node has 2 coordinates. Marginal conditions and loads are applied. The following marginal conditions are preset for the initial analysis: the smallest diameter circle at the corn cob is retained in place. The above marginal conditions are preset in view of the fact that a corn ear is a deformable body which cannot experience the displacement of a rigid body. Nodal forces have been applied to nodes 13, 43 and 55 in view of the physical implication of the task (Fig. 3).

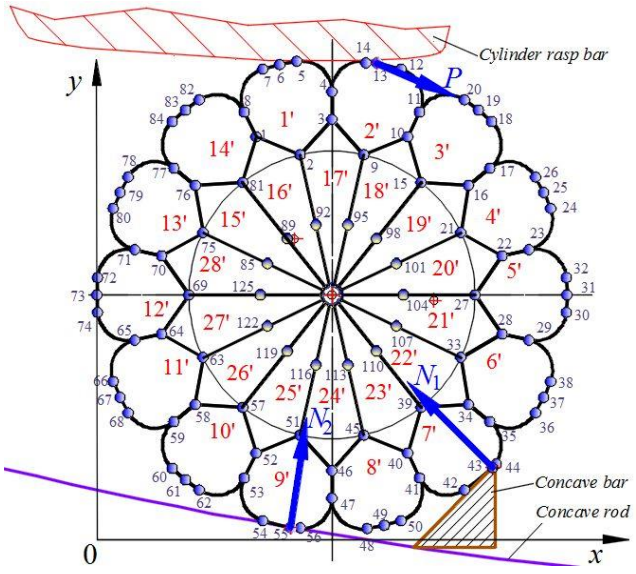

Fig. 5 Corn ear split into isoparametric finite elements: 1'…28' - isoparametric finite elements, 1…127 - nodes

The Matlab R2013a application has been used for the calculations. Calculations with three different concave crossbars (Fig. 2) have been performed. The calculations have involved variation of the numerical value of the corn cob elasticity modulus E within the range of 20 MPa to 35 MPa (by 5 MPa increments), while grain E has been subjected to variation from 80 MPa to 140 MPa in increments of 20 MPa.

The designed model can be used to calculate the effect of loads of different values and directions on the individual parts of a corn ear, depending on the physical

properties of the parts by varying the grain and cob elasticity modulus and Poisson's ratio. The calculation results can be used to determine the displacement of node only the outer, but also inner points of the corn ear.

Nodal displacements and stresses at the preset grain and cob elasticity modulus and Poisson's ratio, which, in radial compression, is equal to 0.32, have been calculated [17]. The red dashed line represents the initial corn ear, black line – deformed corn ear (Fig. 6).

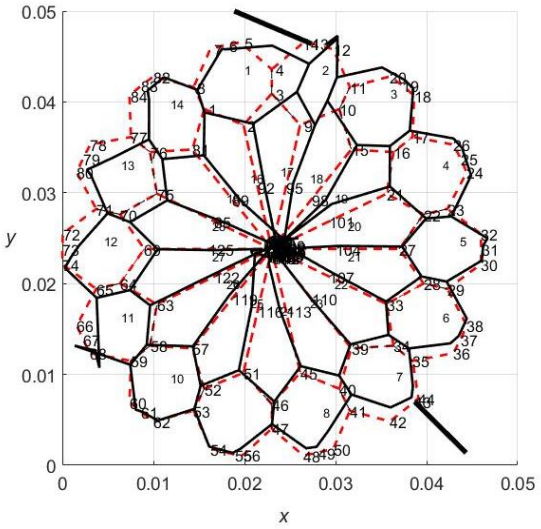

Fig. 6 Corn ear finite elements before (dashed line) and after (full line) the action of external forces

Analysis of the displacements of all fourteen nodes connecting every grain to the corn cob has demonstrated that the displacement of node 63 is the most significant. It can therefore be suggested that as soon as the corn ear is subjected to an action by the rasp bar, grain 11 will become the first grain detached from the cob. Thus, the radial displacement of node 63 from the cob centre can be used for measurement of the efficiency of the crossbar shape. This node is referred to as the corn ear rachilla, which connects the grain to the cob structure. When pulling a grain from the cob, failure of the rachilla occurred. Experimental research using an INSTRON 5960 machine has determined that a 2–3 mm displacement is required for grain detachment by pulling it away from the cob (a more specific amount of displacement depends on the grain and cob moisture content and their elasticity modulus). Theoretical research using the FEM referred to above have shown that displacement of the corn ear rachilla depends on the concave crossbar shape (Table 3). An increase of the grain and cob elasticity modulus leads to a smaller displacement of node 63, but it is sufficient for the separation of grain 11 from the cob only if an oblique concave crossbar is used. In the case of a rectangular crossbar, the displacement of node 63 does not even reach a single millimetre.

Table 3

The effect of the concave crossbar shape on the displacement of the corn ear rachilla (node 63)

Grain *E*, MPa	Crossbar shape		
	Oblique	Rectangular	Rounded edge
	Node 63 displacement, mm		
80	Cob *E* = 20, MPa		
	5.72	0.47	2.33
100	Cob *E* = 25, MPa		
	4.58	0.38	1.86
120	Cob *E* = 30, MPa		
	3.81	0.31	1.55
140	Cob *E* = 35, MPa		
	3.27	0.33	1.33

3. Experimental research methodology

The method of the experiment has been applied for verification of the adequacy of the designed theoretical models. A theoretical analysis is known to usually involve a series of simplifications. Researchers who have analysed the corn ear threshing process have noticed that the interactions are not formed between the ears of corn with fewer ears in the threshing space, thus, the random motion of the corn ears leads to a certain difference between the numerical results and experimental data [13]. The experimental research was conducted in 2015 at the Laboratory for Analysis of Technological Processes of Agricultural Machinery using a stationary tangential single-cylinder threshing stand designed and manufactured specifically for this purpose (Fig. 7).

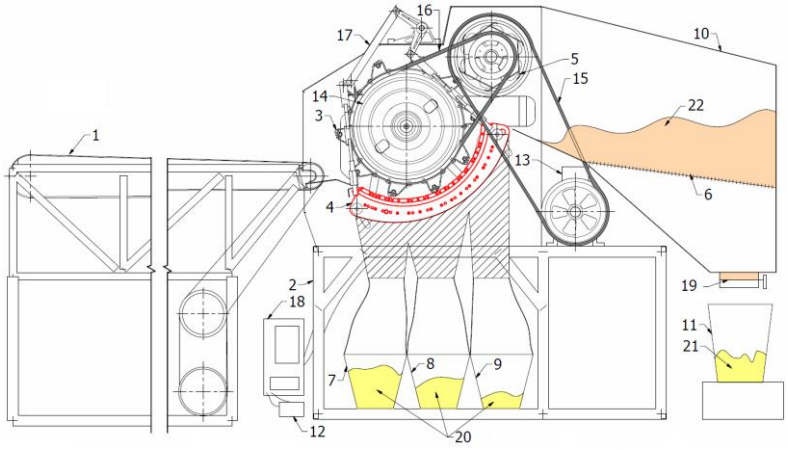

Fig. 7 Corn ear threshing stand: *1* - belt conveyor; *2* - frame; *3* - threshing cylinder; *4* - concave; *5* - beater; *6* - sieve; *7*, *8*, *9*, *10* - containers; 11 - grain box; *12* - supply current, voltage and power meter; *13* - power motor; *14* - belt variator; *15*, *16* - motor, beater and threshing cylinder belt gear; *17* - concave adjustment mechanism; *18* - variable frequency drive, *19* - valve; *20* - grain-chaff mixture; *21* - grain on the walkers; *22* - threshed material

A laboratory shelling device was constructed from conventional combine parts. The stand was comprised of a 10 m long and 0.8 m wide belt conveyor *1* for feeding of the corn ear flow into the threshing unit, and a 1.5 m wide and 0.8 m diameter tangential threshing cylinder *3* with 10 rasp bars (the corn ears were only fed into the 0.8 m wide central section of the threshing unit).

The threshing cylinder was wrapped with a grate concave *4* at a 130° angle. The threshed material with unseparated through concave grains are forwarded to the collecting container *10* by means of the beater *5*. The grain-chaff mixture which entered the open sections of the concave is collected in containers *7*, *8* and *9*.

To bring the working parts of the threshing stand into rotation, a 30 kW power motor was used. Cylinder rotation speed (350 min^{-1}) was set by a Delta VFD-C2000 SERIES variable frequency drive and the belt variator. Cylinder shaft rotation speed was measured by a Chauvin® Arnoux C.A. 1727 digital tachometer.

The crossbars of three different shapes (Fig. 2) to be installed into the variable radius concave (Fig. 8) were designed and manufactured for the research. The crossbars of the shapes depicted in the Fig. 2 a, b and c sections were installed in the concaves with 62.5 mm clearances between them. Then, the concaves were fitted with 14 crossbars each.

Fig. 8 Concave

Before the tests were launched, the clearance between the threshing cylinder rasp bar and concave crossbar was measured: front – 36 mm, middle – 29 mm, rear – 24 mm. Full ripeness *Rodni* variety corn ears were used with the moisture content of grains – 36.36 ± 0.17%, cobs – 60.04 ± 2.09%, tassels – 39.68 ± 5.64%, stalks – 64.30 ± 5.75%, husk leaves – 39.96 ± 7.56%, and were threshed at the threshing stand. After weighing on electronic scales (CAS DB-1H with a maximum capacity of 60 ± 0.02 kg, minimum capacity 400 ± 20 g), the corn ears were spread evenly on a 7 m long conveyor belt and fed into the tangential threshing unit at the speed of 1.0 m s^{-1}. The tests were also conducted by feeding the flow of corn ears into the threshing unit at 9 kg s^{-1}. If the flow had been fed into the entire cylinder (1.5 m) instead of the 0.8 m wide cylinder section, this would have corresponded to a 16.8 kg s^{-1} feed rate.

The tests were repeated 4 times each. The measurement data were assessed by calculating the confidence interval on the mean at 95% probability.

Three samples, each 200 g, were taken from containers *7*, *8*, *9*, and the threshed grain container *11* (Fig. 8) each for determination of damage to the grains. Samples from each container were poured into individual bags tagged with the reference number and the technological parameter subjected to variation. Three samples (100 g each) were separated at the laboratory from each grain bag by division. The grains showing mechanical damage were separated from each sample and weighed. The grain damage was determined by a careful visual inspection of the samples. The percentage share of the average degree of grain damage per each sample was calculated.

The active power required for the rotation of the threshing cylinder was measured using an electric power system analysis device ME-MI2492 (Metrel). The measurement range of the device was 0–150 kW, with a scale-interval value of 0.1 kW, and the power measurement error was ± 3% of the measured value. Afterwards, the total power consumption for threshing the corn ears was found. Besides the application of the Metrel device, measurements of the current and voltage necessary for the rotation of the electric motor were performed using an Almemo 2890-9 device simultaneously. The availability of the data enabled the authors to calculate power consumption.

4. Experimental test results

Grain separation loss is the key parameter used to evaluate the performance of combine harvesters, and also a dominant factor for adjusting their major working parameters [18]. Concave separation efficiency is defined as the proportion of threshed grains which pass through the concave rather than over the rear of the concave. The tests have demonstrated that replacement of the crossbars in the first concave section may lead to an increase of grain separation from 26.23 ± 2.95% (rectangular crossbars) to 40.87 ± 2.80% (oblique crossbars β = 45°) (Fig. 9).

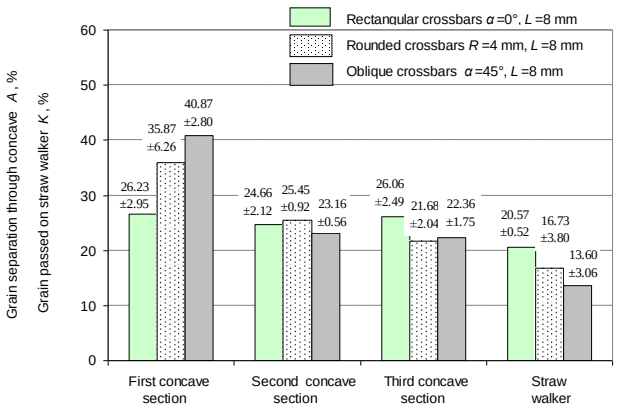

Fig. 9 The effect of the concave crossbar shape on grain separation

For any shape of the crossbar in the second concave section, grain separation varied within a fairly narrow range of 23.16 ± 0.56% to 25.45 ± 0.92%. In terms of the most efficient crossbar shape in terms of grain separation through the third concave section, rectangular crossbars (26.06 ± 0.49%) have provided the best results. 13.60 ± 3.06% to 20.57 ± 0.52% grains have been found to reach the straw walkers when using different shapes of crossbars (Fig. 9). The best grain separation results were provided by the concave with oblique crossbars, β = 45°, and this shape of crossbars has also been characterised by the smallest share of grains (13.60 ± 3.06%) resulting on the straw walkers. Moreover, oblique crossbars provide almost no threshing losses (Table 4). Threshing losses are

grains that remain on the cob due to incomplete cylinder action.

The problem of corn grain damage is important and large in scope. Field shelling causes most of the mechanical damage to the grain, largely due to the high moisture content, and the harvesting and technological parameters [3]. In terms of damage to the grains, the lowest degree of damage has been noticed from $1.16 \pm 0.32\%$ to $1.97 \pm 0.38\%$ in the first concave section. The difference between the power demands required to support cylinder rotation during corn ear threshing using rectangular, rounded or oblique crossbars is not significant – approx. 1 kW, i.e. approx. 6%. Nevertheless, the uniformity in the variation of the power demand measured on the confidence interval of the arithmetic mean under the established operating mode is considerably higher when using oblique concave crossbars (Table 4).

Table 4

The effect of the concave crossbar shape on damage to the grains, threshing losses and threshing power demand

Crossbar shapes	Grain damage S, %				Threshing losses N, %	Power consumption Q, kW
	First concave section	Second concave section	Third concave section	On the straw walkers		
Rectangular, L=8 mm	1.97 ± 0.38	3.00 ± 0.63	3.58 ± 0.58	4.90 ± 1.40	2.08 ± 1.80	16.91 ± 2.94
Rounded, L=8 mm	1.42 ± 0.33	3.01 ± 0.33	4.08 ± 1.02	4.33 ± 0.53	0.32 ± 0.21	17.79 ± 1.75
Oblique α=45°, L=8 mm	1.16 ± 0.32	2.11 ± 0.50	3.22 ± 0.70	4.64 ± 0.59	0.03 ± 0.01	17.98 ± 0.36

The theoretical analysis and experimental tests have demonstrated that use of the concave with oblique crossbars, $\beta = 45°$, generates better values for all the parameters of the threshing process compared to the other two shapes of crossbars; however, the oblique crossbars would probably be subjected to more rapid wear during prolonged operation. It would therefore be reasonable to focus further experimental tests on a determination of the effect of oblique crossbars wider than 8 mm and having a smaller angle than 45° β (e.g., 35°) on the efficiency of the corn ear threshing.

5. Conclusions

1. A numerical analysis of the corn ear threshing process has been conducted, and a mathematical model of the corn ear threshing has been developed. A process calculation scheme has been developed for the static equilibrium analysis and the numerical values of the reaction forces in the threshing process have been determined. The efficiency of the threshing process has been found to depend on the geometrical shapes of the concave crossbars. Substantiation of the rationale behind the use of a oblique concave cross bar, with a working plane tilt angle ranging between 35° and 40°, has been provided.

2. The mathematically flexible finite element method involving the application of curved isoparametric second order finite elements with Serendip type shape functions adapted to the study has been proposed for similar studies. This method enables the researchers to analyse the response of the individual parts of an ear in consideration of the various force effects. The displacement and deformation values have been found to depend on the elasticity modulus of the corn ear grains and cob.

3. The experimental tests have demonstrated that replacement of the concave crossbar shapes may result in a more efficient separation of grains through the concave, a lower share of grains resulting on the straw walkers, and less damage to the grains as well as lower threshing losses.

4. The conducted research has provided substantiation for the conclusions of the theoretical analysis suggesting that a variable radius concave with a working plane tilt angle of the oblique crossbar equal to 45° would be the most rational option for corn ear threshing. In this case, the threshing losses of the grains are minimal ($0.03 \pm 0.01\%$), and the maximum share of grains damaged in the threshing unit does not exceed 4%.

References

1. World Agricultural Production. Foreign Agricultural Service, FAS, USDA [online]. Circular Series WAP 9-16. September 2016 [accessed 16 Sept. 2016]. Available from Internet: http://apps.fas.usda.gov/psdonline/circulars/production.pdf.
2. **Yang, L.; Cui, T.; Qu, Z.; Li, K.; Yin, X.; Han, D.; Yan, B., Zhao, D., Zhang, D.** 2016. Development and application of mechanized maize harvesters, International Journal of Agricultural and Biological Engineering 9(3): 15-28. http://dx.doi.org/10.3965/j.ijabe.20160903.2380.
3. **Miodragovic, R.; Djevic, M.** 2006. Contemporary combine harvesters in corn harvesting, Annals of the Faculty of Engineering Hunedoara: 4(3): 199-206.
4. **Poničan, J.; Angelovič, M.; Jech, J.; Žitnak, M.** 2007. Effects of kinematic parameters of combine harvester on maize grain quality, Contemporary Agricultural Engineering 33(3-4): 135-142.
5. **Yu, Y.; Yu, J.; Li, Q.; Yu, J.; Fu, H.** 2013. Analysis on the contact interaction between thresher and corn ears based on the DEM, Applied Mechanics and Materials 246-247: 71-77. http://dx.doi.org/10.4028/www.scientific.net/AMM.246-247.71.
6. **Miu, P.I.** 2015. Cereal threshing and separating processes: threshing units, In: Miu, P. (ed.) Theory, Modelling, and Design. CRC Press, 189-260. http://dx.doi.org/10.1201/b18852-6.
7. **Norris, E.R.; Wall, G.L.** 1986. Effect of concave de-

sign factors on cylinder-concave performance in corn, Canadian Agricultural Engineering 28(2): 97-99.
8. **Pužauskas, E.** 2016. The concave for threshing machines of cereal crops. Patent. WO 2016048124.
9. **Rakauskas, K.; Pužauskas, E.; Steponavičius, D.** 2015. The influence of concave design on grain separation and damage, Agroinžinerija ir Energetika 20: 18-25.
10. **Poničan, J.; Angelovič, M.; Jech, J.; Žitňák, M.; Findura, P.** 2009. The effect of the design concept of combine harvester threshing mechanism on the maize crop threshing quality, Contemporary Agricultural Engineering 35(4): 268-274.
11. **Tiwari, P.S.; Pandey, M.M.; Gite, L.P.; Shrivastava, A.K.** 2010. Effect of operating speed and cob size on performance of a rotary maize sheller, Journal of Agricultural Engineering 47(2): 1-8.
12. **Petkevičius, S.; Steponavičius, D.; Pužauskas, E.** 2012. Grain separation from pith under quasi-static radial compression of corn ear, In: Proceedings of the 17th International Conference Mechanika-2012, Kaunas, Lithuania, 224-228.
13. **Yu, Y.; Fu, H.; Yu, J.** 2015. DEM-based simulation of the corn threshing process, Advanced Powder Technology 26: 1400-1409. http://dx.doi.org/10.1016/j.apt.2015.07.015.
14. **Markauskas, D.; Ramírez-Gómez, Á.; Kačianauskas, R.; Zdancevičius, E.** 2015. Maize grain shape approaches for DEM, Computers and Electronics in Agriculture 118: 247-258. http://dx.doi.org/10.1016/j.compag.2015.09.004.
15. **Xu, L.; Li, Y.; Ma, Z.; Zhao, Z.; Wang, C.** 2013. Theoretical analysis and finite element simulation of a rice kernel obliquely impacted by a threshing tooth, Biosystems Engineering 114: 146-156. http://dx.doi.org/10.1016/j.biosystemseng.2012.11.006.
16. **Barauskas, R.; Belevičius, R.; Kačianauskas, R.** 2004. The Basics of the Finite Elements Method, Vilnius: Technika, 612 p. (in Lithuanian).
17. **Anazodo, U.G.N.; Wall, G.L.; Norris, E.R.** 1981. Corn physical and mechanical properties as related to combine cylinder performance, Canadian Agricultural Engineering 23(1): 23-30.
18. **Liang, Z.; Li, Y.; Zhao, Z.; Xu, L.** 2015. Structure optimization of a grain impact piezoelectric sensor and its application for monitoring separation losses on tangential-axial combine harvesters, Sensors 15: 1496-1517. http://dx.doi.org/10.3390/s150101496.

E. Pužauskas, D. Steponavičius, E. Jotautienė,
S. Petkevičius, A. Kemzūraitė

SUBSTANTIATION OF CONCAVE CROSSBAR SHAPE FOR CORN EAR THRESHING

S u m m a r y

One of the key design parameters of a threshing unit critical for corn ear threshing is the shape, height and number of the concave crossbars. The paper presents the results obtained during the theoretical and experimental research of corn ears threshing process by analysing the crossbars of three different shapes: rectangular, rounded and oblique. The FEM involving the application of curved isoparametric second order finite elements with Serendip type shape functions was adapted to this research. The method of the experiment has been applied for verification of the adequacy of the designed theoretical models. The theoretical and experimental analysis has demonstrated that oblique concave crossbars were more efficient during threshing of corn ears that using any of the other two shapes of crossbars. The experimental research has substantiated that a variable radius concave with a working plane tilt angle of the oblique crossbar equal to 45° would be the rational option for corn ear threshing. In this case, the threshing losses and grain damage were least.

Keywords: combine harvester, threshing cylinder, concave, corn ear, grain separation, grain damage.

Received October 06, 2016
Accepted December 02, 2016